



Published in final edited form as:

Prog Biophys Mol Biol. 2016 July ; 121(2): 185–194. doi:10.1016/j.pbiomolbio.2016.06.004.

Computational Rabbit Models to Investigate the Initiation, Perpetuation, and Termination of Ventricular Arrhythmia

Hermenegild J. Arevalo, Ph.D.^{1,2}, Patrick M. Boyle, Ph.D.¹, and Natalia A. Trayanova, Ph.D.¹

¹Department of Biomedical Engineering, Johns Hopkins University, Baltimore, MD

²Simula Research Laboratory, Oslo, Norway

Abstract

Current understanding of cardiac electrophysiology has been greatly aided by computational work performed using rabbit ventricular models. This article reviews the contributions of multiscale models of rabbit ventricles in understanding cardiac arrhythmia mechanisms. This review will provide an overview of multiscale modeling of the rabbit ventricles. It will then highlight works that provide insights into the role of the conduction system, complex geometric structures, and heterogeneous cellular electrophysiology in diseased and healthy rabbit hearts to the initiation and maintenance of ventricular arrhythmia. Finally, it will provide an overview on the contributions of rabbit ventricular modeling on understanding the mechanisms underlying shock-induced defibrillation.

Keywords

ventricular arrhythmia; cardiac electrophysiology; defibrillation; computational modeling; ischemia; myocardial infarction

I. Introduction

The rabbit animal model is used extensively in experimental cardiac electrophysiological studies due to its lower housing costs compared to larger animals (eg., dogs, sheep, pigs) while simultaneously providing a reasonable approximation of human cardiac electrophysiological activity compared to smaller animals (eg rats, mice, guinea pigs). Rabbit cardiac electrophysiological characteristics have been shown to reasonably match the human's in terms of the relationship between wavelength and cardiac size (Hill et al., 2013), the presence of a strong transient outward Ito current (Varró et al., 1993), as well as the similar dynamics of the repolarizing IKr and IKs currents (Husti et al., 2015; Zicha et al., 2003).

Corresponding Author: Natalia A. Trayanova, Ph.D., Johns Hopkins University, 3400 N Charles St, 216 Hackerman Hall, Baltimore, MD 21218, USA, Phone: +1 410-516-4375, Fax: +1 410-516-5294, ntrayanova@jhu.edu.

Editors' note: Please see also related communications in this issue by Gemmell et al. (2016) and Teh et al. (2016).

Publisher's Disclaimer: This is a PDF file of an unedited manuscript that has been accepted for publication. As a service to our customers we are providing this early version of the manuscript. The manuscript will undergo copyediting, typesetting, and review of the resulting proof before it is published in its final citable form. Please note that during the production process errors may be discovered which could affect the content, and all legal disclaimers that apply to the journal pertain.

Over the past ~35 years, computational modeling has emerged as an important tool that can explain cardiac electrophysiological mechanisms that cannot be easily elucidated from experimental techniques alone. To complement the use of rabbit ventricles in experimental studies, much effort has been devoted to the development of computational modeling tools and techniques for representing the electrophysiology of the rabbit heart at the cell, tissue, and organ scales. The focus of this paper is to summarize recent contributions of studies utilizing computational models of the rabbit ventricles in uncovering the mechanisms of arrhythmia induction, maintenance, and termination. The works reviewed below developed and utilized rabbit ventricular models of various complexity, in healthy and diseased states, to advance the understanding of how structural and electrophysiological heterogeneities affect cardiac electrical function.

II. Multi-scale building blocks for modeling rabbit cardiac electrophysiology

At the cell scale, the basic units of computational electrophysiology are action potential (AP) models, which describe membrane kinetics via coupled systems of nonlinear ordinary differential equations (ODEs). These equations represent current flow through ion channels, pumps, and exchangers as well as subcellular calcium cycling and are solved to observe how states (transmembrane potential $[V_m]$ and ionic concentrations) evolve over time as they interact with one another and respond to perturbations. Many rabbit-specific models have been developed, with variants representing the behavior of several different parts of the heart, all of which provide important building blocks for the execution of realistic multi-scale simulations.

The first rabbit-specific AP model for ventricular myocytes was developed by Puglisi and Bers (Puglisi and Bers, 2001). In subsequent years, this model was carefully refined to incorporate a more realistic representation of high-gain Ca^{2+} -induced Ca^{2+} release from the sarcoplasmic reticulum (Shannon et al., 2004) and to reproduce the emergence of Ca^{2+} transient alternans during rapid pacing (Mahajan et al., 2008; Romero et al., 2011). Models from this lineage have been used subsequently to demonstrate that execution of simulations with a range of conductance values for repolarizing currents results in the reproduction of physiologically relevant variability in rabbit ventricular AP shape (Fig. 1A) (Gemmell et al., 2014). A more recent innovation has been the development of rabbit-specific AP models geared towards representing specialized cells of the atrioventricular node (AVN) and penetrating His bundle (Inada et al., 2009) as well as fibers of the Purkinje system (PS) (Aslanidi et al., 2010; Corrias et al., 2011).

A smaller number of studies have even attempted to characterize tissue-scale electrophysiological properties in rabbit hearts. For example, Tice et al. developed a slice model of the rabbit ventricles with regional phase 1A ischemia by incorporating realistic transmural gradients in extracellular potassium concentration ($[K^+]_o$), ion channel expression, and adenosine triphosphate (ATP) availability (Tice et al., 2007).

Finally, at the organ scale, numerous groups have published detailed descriptions of the macroscopic geometry of the rabbit ventricles. A seminal example is the work of Vetter and

McCulloch, who cast the rabbit myocardium in dental rubber and then analyzed the full stack of 2-3 mm-thick short-axis slices to produce a 3-dimensional reconstruction of ventricular geometry including a detailed description of myofiber architecture (Vetter and McCulloch, 1998). The same ventricular geometry (sometimes called the UC San Diego rabbit heart) has been re-discretized by several different groups (Fig. 1B) (Boyle et al., 2010; Deo et al., 2013; Fenton et al., 2005; Hill et al., 2016; Meunier et al., 2002; Sampson and Henriquez, 2005) and used in a majority of the computational studies of rabbit ventricular electrophysiology described elsewhere in this review. More recently, the advent of powerful new magnetic resonance imaging (MRI) tools has enabled the reconstruction of even more detailed cardiac models, such as the rabbit ventricular model developed as part of the Oxford 3D Heart Project (Bishop et al., 2010b; Burton et al., 2006; Vadakkumpadan et al., 2010; Vadakkumpadan et al., 2009). Such MRI-based models are sufficiently high-resolution (25 μm) that is possible to incorporate detailed representations of fine-grain anatomical features such as blood vessels, endocardial trabeculations, and fibrous tissue bundles. Diffusion tensor MRI, which measures diffusivity of water in the tissue, has been used to obtain accurate representation of fiber architecture in the rabbit ventricles (Benson et al., 2008; Higham et al., 2011; Krishnamoorthi et al., 2014). Moreover, heterogeneous AP properties can be assigned to histologically distinct regions (e.g., PS fibers), which can be manually or automatically segmented via image processing techniques (Fig. 1C) (Bishop et al., 2010b; Vadakkumpadan et al., 2009). Finally, organ-scale models of several components of the rabbit's specialized conduction system have been developed and coupled with ventricular models for use in computational studies aiming to study the AVN (Inada et al., 2009) and the PS (Atkinson et al., 2011; Behradfar et al., 2014; Bordas et al., 2011; Boyle et al., 2010; Vigmond and Clements, 2007).

III. Initiation and Perpetuation of Ventricular Arrhythmia

a) Contributions of the Cardiac Conduction System

In addition to its critical role in the coordination of ventricular excitation, the PS has been implicated as a factor in the initiation and maintenance of arrhythmias, including catecholaminergic polymorphic ventricular tachycardia (CPVT) (Cerrone et al., 2007) and idiopathic ventricular fibrillation (Haissaguerre et al., 2002; Hooks et al., 2015). However, complete understanding of these contributions has been elusive because bioelectric activity in the PS must be inferred from low-amplitude electrograms (Robichaux et al., 2010). Consequently, computational simulations have been an important driver for improving understanding of PS-related arrhythmias in the past decade. Rabbit models have been particularly useful in this context due to similarities between human and rabbit arrhythmia dynamics (Panfilov, 2006) and PS geometric structure (unlike in dogs, pigs, and larger ungulates, human and rabbit PS fibers barely penetrate the endocardial surface) (Coghlan et al., 2006; Trandum-Jensen et al., 1991).

One of the most recent findings facilitated by simulation-based research involving a rabbit model is that stochastically-timed cell-scale Spontaneous Calcium Release (SCR) events in the PS are much more likely to overcome source-sink imbalance and trigger organ-scale Premature Ventricular Contractions (PVCs) compared to SCRs occurring in the electrically

well-coupled myocardium (Campos et al., 2015). Even though the number of ventricular cells was ~ 2 orders of magnitude larger than the number of PS fibers, all ectopic foci observed in this study occurred in the PS, without exception, with the majority ($\sim 68\%$) occurring within 1 mm of a Purkinje-myocardial junction (PMJ) (Fig. 2A). Using a similar model, Zamiri et al. showed that delayed afterdepolarizations elicited propagating APs in the PS but not in the myocardium (Fig. 2B) and demonstrated that simulated application of the RYR-2 blocker Dantrolene to the PS alone was adequate to completely extinguish these potentially pro-arrhythmic excitations (Zamiri et al., 2014). In a related study, Baher et al. used a rabbit model to demonstrate that alternating excitation of the left and right sides of the PS (driven by reciprocating ectopic foci) produced a bidirectional ECG consistent with patterns seen in CPVT patients (Baher et al., 2011).

A related research trajectory is the use of rabbit computational models to better understand how the distinct topological structure and electrophysiology of the PS can contribute to the substrate for initiation and perpetuation of various types of reentrant arrhythmia. Simulation studies have shown that a single ectopic beat originating in the PS can initiate reentry (Deo et al., 2010) and that the dynamics of reentrant wavefront propagation in ventricular tissue can be strongly influenced by electrical interaction with coupled tissue in the PS (Boyle et al., 2013a; Deo et al., 2009). Effects observed in the latter studies include rotor stabilization due to refractoriness around PMJs, wavebreak caused by excitation emerging from the PS, rapid shunting of activation between distant ventricular sites via PS propagation, and increased spatial heterogeneity of left ventricular activation rate due to breakthroughs from the PS.

Lastly, rabbit models have been used to better understand how PS contributions might affect the treatment of heart rhythm disorders. For example, early excitations caused by field-induced depolarization of PS fibers have been shown to accelerate ventricular activation in response to weak electric shocks by up to $\sim 30\%$ (Boyle et al., 2010). Modeling research has also shown that retrograde excitation of the PS via pacing-induced wavefronts can lead to faster than expected organ-scale activation in the context of cardiac resynchronization therapy (Romero et al., 2010) or complicate diagnostic differentiation between orthodromic reciprocating tachycardia and other forms of supraventricular arrhythmia (Boyle et al., 2013b). Simulations in rabbit models were also used to explore low-energy arrhythmia termination based on the emerging technology of cardiac optogenetics (Boyle et al., 2013c). Light-based stimulation of the PS via tissue-specific optogenetic targeting was shown to be much more energy efficient than when a similar approach was used to directly excite ventricular tissue.

b) Contributions of Ventricular Geometry

Previous experimental and simulation studies have investigated the effects of heterogeneous ventricular geometry on electrical propagation in the heart (Fast and Kleber, 1995b). In particular, it has been known that sites of tissue expansion could promote conduction block due to source-sink mismatch (Fast and Kleber, 1995a; Xie et al., 2010). The pro-arrhythmic effects of this mechanism was investigated in a computational study using the UCSD rabbit ventricular geometry (Boyle et al., 2014). Boyle et al demonstrated that in structurally

normal ventricles with decreased sodium channel expression, a condition typical in genetic disorders such as Brugada syndrome (Berne and Brugada, 2012), macroscopic geometric heterogeneities can provide the substrate for arrhythmia initiation in the ventricles. They found that PVCs originating from the RV outflow tract failed to propagate through the RV/LV junction and initiated reentry (Fig. 3). Calculating the 3D safety factor (SF), an index that represents conduction robustness by measuring the amount of excess charge delivered from cell to cell, showed that sites where thin RV adjoins thick LV tissue had large regions of critical source-sink mismatch ($SF < 1$). An SF value of less than 1 indicates that not enough charge is available to excite cells and thus conduction block results.

The possible effects of microscopic structural heterogeneity on electrical propagation has also been explored in rabbit ventricles. The Oxford rabbit heart model (Bishop et al., 2010b), constructed from high resolution MRI ($< 20 \mu\text{m}$), accurately captured the complex ventricular geometry including endocardial trabeculations, blood vessels, and papillary muscles. In a series of studies using this model, investigators report that the matrix of endocardial trabeculae and papillary muscles could provide shortcut pathways that altered the overall activation pattern compared to a model that excludes these structural details (Bishop et al., 2010b). In a subsequent study, the same investigators report that these shortcut pathways do not significantly alter propagation during reentrant activity (Bishop and Plank, 2012). However, when chaotic ventricular fibrillation (VF) is induced, the complexity increased in the structurally detailed models, with filaments (the organizing center of reentrant activity) clustering around endocardial structures (Bishop and Plank, 2012). The results of these studies underscore the potentially important role cardiac microstructure could play in determining specific propagation patterns during arrhythmia.

c) Contributions of Intrinsic Electrophysiological Heterogeneity

Electrophysiological heterogeneity due to different regional expression levels of various ionic currents have been known to exist in mammalian ventricles (Antzelevitch and Fish, 2001). This manifest as action potential (AP) morphology differences from endocardium-epicardium (Fedida and Giles, 1991; Idriss and Wolf, 2004; Xu et al., 2001), apex-to-base (Cheng et al., 1999), and LV vs RV (Samie et al., 2001). The effects of these intrinsic AP heterogeneities on arrhythmia initiation and maintenance have been investigated using biventricular models of the rabbit ventricles. A study that incorporated both transmural and apicobasal AP heterogeneity found that in the setting of sustained arrhythmia, the presence of AP heterogeneity did not significantly alter activation patterns or arrhythmia complexity (Bishop et al., 2013). This is due to the effects of electrotonic coupling, which modulated the AP morphology differences, and the fast rate of activation during reentrant activity resulting in shortened AP duration throughout the ventricles. However, the investigators found that the ventricles with AP heterogeneity were more susceptible to regional conduction block and arrhythmia induction during delivery of premature stimuli. In the homogeneous ventricles, delivery of premature stimuli was more likely to result in complete block that failed to initiate arrhythmia.

In the setting of VF, AP heterogeneity has been found to have a significant role in determining the spatiotemporal organization of scroll waves. Modeling studies have shown

that filament stability is sensitive to the presence of heterogeneity, with increased heterogeneity resulting in increased likelihood of filament break-up and increased complexity of VF dynamics (Clayton et al., 2006; Xie et al., 2001). In the normal rabbit ventricles, Arevalo et al demonstrated that the behavior of the filaments was found to depend on AP duration (APD) heterogeneity in the ventricles (Arevalo et al., 2007). The rabbit ventricular model incorporated LV and RV APD heterogeneity due to differences in expression of the inward rectifier current (Samie et al., 2001). The study found that the presence of APD heterogeneity induced a more turbulent VF with increased incidence of conduction block and formation of new reentrant circuits at the RV/LV border (Fig. 4).

d) Contributions of Remodeling Due to Ischemia and Myocardial Infarction

Ventricular remodeling during ischemia and infarction further exacerbate ventricular heterogeneity and directly influence the inducibility and maintenance of arrhythmic activity. During ischemia, decreased perfusion due to coronary occlusion results in hyperkalemia, activation of the ATP-sensitive potassium current, and acidosis (Pinto and Boyden, 1999; Shaw and Rudy, 1997a; Shaw and Rudy, 1997b). Rabbit ventricular models representing regional ischemia (Jie et al., 2008; Jie and Trayanova, 2010) have characterized the substrate for ischemia phase 1B arrhythmias by examining how the interplay between different degrees of hyperkalemia in the surviving layers, and the level of cellular uncoupling between these layers and the mid-myocardium combine with the specific geometry of the ischemic zone in the ventricles to result in reentrant arrhythmias. In a subsequent study, Jie et al. incorporated mechanics into the ischemic rabbit model to gain insight into the potential role of electromechanical dysfunction in post-ischemia induction of premature beats and their degeneration into ventricular arrhythmia (Jie et al., 2010). They found that mechanical stretch in the ischemic region promoted arrhythmia via generation of ventricular premature beats and providing a substrate with slowed conduction due to stretch-related membrane depolarization.

Chronic occlusion of the blood vessels results in irreversible structural and electrical remodeling resulting in formation of infarcted tissue. In addition to the presence of scar tissue and partially viable myocytes in the peri-infarct zone (PZ), infarcted tissue has also been reported to have increased expression of myofibroblasts (Camelliti et al., 2005; Rohr, 2009). Myofibroblasts have been reported to couple to surrounding myocytes and alter myocyte AP morphology (Vasquez et al., 2010). In lower scale simulation studies, myofibroblast coupling has been shown to shorten APD in surrounding myocytes by acting as an electrotonic sink (Ashihara et al., 2012; Jacquemet and Henriquez, 2008; MacCannell et al., 2007; Maleckar et al., 2009a; Maleckar et al., 2009b; Sachse et al., 2008). This effect was further explored by McDowell et al in a novel high resolution MRI-based model of infarcted rabbit ventricles that incorporated accurate representation of scar and PZ architecture (Fig. 5) (McDowell et al., 2011). In the study, the authors incorporated differing degrees of myofibroblast infiltration into the PZ. They found that the presence of myofibroblasts at low densities did not alter ventricular propensity to arrhythmia. At intermediate intensities, the myofibroblast induced APD shortening in the PZ region that increased APD dispersion and led to increased vulnerability to reentry. Interestingly, further increasing myofibroblast density was found to be protective against arrhythmia induction.

While the extent of myofibroblast differentiation and infiltration in infarcted hearts as well as the level of electrical coupling between myocytes and fibroblasts remain not fully understood, this work highlights the possible mechanisms of increased arrhythmia vulnerability in infarcted hearts.

e) Contributions of Mechanoelectric feedback

One of the first attempts to computationally investigate the role of mechanoelectric feedback on arrhythmia mechanisms was performed by Li et al. in rabbit ventricles. They developed a pseudo-electromechanical models of the rabbit ventricles that incorporated stretch activated channels (SAC) to represent the effects of mechanical stimulation (Li et al., 2008; Li et al., 2004; Li et al., 2006; Trayanova et al., 2004). In this simplified model, mechanical stretch resulted in the opening of SACs and hyperpolarization. Modeling real world mechanical stimuli such as impact from baseballs, the investigators provided insights into the mechanisms by which regional impact to the chest can lead to the induction of arrhythmias via heterogeneous recruitment of stretch activated channels (Li et al., 2004). They found that an appropriately sized mechanical force delivered at a narrow time window during sinus rhythm could induce arrhythmia in a normal heart. They further extended the application of pseudo-electromechanical modeling to investigate the role of stretch on arrhythmia termination via the precordial thump (Li et al., 2006) as well as defibrillation (Li et al., 2008; Trayanova et al., 2004).

IV. Termination of Ventricular Arrhythmia

a) Elucidating Mechanisms of Defibrillation

The most effective therapy for turbulent VF remains the delivery of an electric shock via external or implanted electrodes. Over the years, rabbit ventricular models of defibrillation have made significant contributions to understanding how defibrillation shocks interact with cardiac tissue (Aguel et al., 2003; Arevalo et al., 2007; Ashihara and Trayanova, 2004; Bourn et al., 2006; Hillebrenner et al., 2004; Maharaj et al., 2008; Maleckar et al., 2008; Meunier et al., 2002; Plank et al., 2008; Rodriguez et al., 2006; Rodriguez et al., 2005; Tandri et al., 2011; Trayanova et al., 1998). In particular, these models have been instrumental in the development of the virtual electrode polarization (VEP) theory for defibrillation (Efimov et al., 2000; Efimov et al., 1998; Trayanova et al., 1998). These studies have found that defibrillation shock success or failure depends on the pre-shock distribution of transmembrane potential as well as the timing and location of shock-induced wavefronts. In addition, recent simulation studies have helped understand the mechanisms of the isoelectric window that follows defibrillation shocks with strength near the defibrillation threshold (DFT): one of the proposed explanations for the isoelectric window duration is propagation of postshock activations in intramural excitable areas (“tunnel propagation”), bounded by long-lasting postshock depolarization of the cardiac surfaces. (Ashihara et al., 2008; Constantino et al., 2010). Ventricular simulations using a section of the high resolution Oxford rabbit model have also given insights into the possible role of cardiac microstructure in the mechanisms of defibrillation (Bishop et al., 2010a). The investigators found that applied shock resulted in the formation of VEPs at the boundaries between blood

vessels and myocardium. The VEPs elicited the formation of wavefronts that propagated through excitable gaps and led to successful defibrillation (Bishop et al., 2012).

Rabbit ventricular models have also been used to elucidate the mechanisms of defibrillation in ischemic and infarcted hearts (Rantner et al., 2012; Rodriguez et al., 2004b; Rodriguez et al., 2004c). Rodriguez et al used the UCSD rabbit ventricle model to examine the role of electrophysiological remodeling during different phases of global acute ischemia in determining success or failure of defibrillation shocks (Rodriguez et al., 2004a; Rodriguez et al., 2004b; Rodriguez and Trayanova, 2003). Vulnerability grids were then constructed to determine the upper limit of vulnerability (ULV), the stimulus strength above which the shock cannot induce arrhythmia. The ULV has been shown to correlate with the DFT, which is the minimum energy required for successful cardioversion (Chen et al., 1986). Rodriguez et al found that within 2-3 minutes post-ischemia, ULV did not differ from the normoxic value. As ischemia progressed, they found that the hearts became less vulnerable to shocks resulting in decreased ULV. Uncovering the mechanisms responsible for this behavior showed that changes in the ULV were due to an increase in the spatial extent of shock-end excitation wavefronts, and the slower recovery from shock-induced positive polarization.

Modeling also provided insights into the potential underlying mechanisms determining increased vulnerability to shocks in infarcted hearts. Using the same high resolution MRI-based model of infarcted rabbit ventricles used by McDowell et al (McDowell et al., 2011) and enriched with optical mapping data (Bishop et al., 2007b; Li et al., 2009), Rantner et al investigated the role of the presence of the infarct scar and PZ in determining the ULV (Rantner et al., 2012). They found that infarcted hearts had a significantly higher ULV (8 V/cm) vs the control model which represented the ventricles as electrophysiologically homogeneous (4 V/cm). Mechanistically, the increase in ULV was due to weaker shock-induced depolarization around the infarct which provided larger areas of excitable tissue for post-shock propagation (Fig. 6). In addition, delayed post-shock activation within the PZ provided a source for wavefronts that propagated through the excitable tissue and thus perpetuate arrhythmia.

b) Exploring New Methods for Defibrillation

Recently, defibrillation modeling has focused on the development of new methodologies for low-voltage termination of lethal arrhythmias or for applying defibrillation in novel, less damaging ways. The study by Tandri et al. (Tandri et al., 2011) used sustained kilohertz-range alternating current (AC) fields for arrhythmia termination. Termination of arrhythmia with AC fields has been attempted previously in simulations (Meunier et al., 2002; Meunier et al., 1999; Meunier et al., 2001) with limited success; the frequencies used in these studies were, however, substantially lower. The premise of the Tandri et al. study was that such fields have been known to instantaneously and reversibly block electrical conduction in nerve tissue. Aided by ventricular modeling, the article provided proof of the concept that electric fields, such as those used for neural block, when applied to cardiac tissue, similarly produce reversible block of cardiac impulse propagation and lead to successful defibrillation; it also showed that this methodology could potentially be a safer means for terminating life-threatening reentrant arrhythmias. Since the same AC fields block equally

well both neural and cardiac activity, the proposed defibrillation methodology could possibly be utilized to achieve high-voltage yet painless defibrillation. The follow-up study by Weinberg et al. (Weinberg et al., 2013) provided, again using ventricular simulations, a deeper analysis of the mechanisms that underlie the success and failure of this novel mode of defibrillation.

Recent experimental studies have shown that applied electric fields delivering multiple far-field stimuli at a given cycle length can terminate VT, atrial flutter, and atrial fibrillation with less total energy than a single strong shock (Li et al., 2011; Li et al., 2009; Luther et al., 2011). However, the mechanisms and full range of applications of this new mode of defibrillation have remained poorly explored. The recent simulation study by Rantner et al. aimed to elucidate these mechanisms and to develop an optimal low-voltage defibrillation protocol (Rantner et al., 2013). Based on the simulation results using a complex high-resolution MRI-based ventricular wall model, a novel two-stage low-voltage defibrillation protocol was proposed that did not involve the delivery of the stimuli at a constant cycle length. Instead, the first stage converted VF into VT by applying low-voltage stimuli at instants of maximal excitable gap, capturing large tissue volume and synchronizing depolarization. Fig. 6 illustrates this approach; in this case the applied far-field pulse train directly terminated VF. The second stage was designed to terminate VT, in cases where it persisted, by multiple low-voltage stimuli given at constant cycle lengths. The energy required for successful defibrillation using this protocol was 57.42% of the energy for low-voltage defibrillation when stimulating at the optimal fixed-duration cycle length.

V. Mechanistic Understanding of Optical Mapping

The development of rabbit ventricular models has been greatly aided by the abundance of electrophysiological data on healthy and diseased rabbit hearts which can be used to validate model predictions. Most of these data were obtained via optical mapping which uses voltage-sensitive fluorescent dyes to measure electrical activity on the surface of the heart (Efimov et al., 2004; Gray et al., 1998; Mironov et al., 2008). However, inherent properties of light and myocardium results in photon scattering and distortion of the recorded signal. To understand how photon scattering can affect the interpretation of optical mapping data, Bishop et al used a rabbit ventricular model combined with a 3D model of photon scattering in a series of simulation studies (Bishop et al., 2007a; Bishop et al., 2006; Bishop et al., 2007b). The models demonstrated that due to photon scattering, the signals recorded via optical mapping on the surface of the heart were actually an amalgamation of signals within a volume of tissue. The level of distortion depended on the geometry of the tissue, direction of wave propagation, and specifics of the experimental setup. The simulations also found that aberrations in optical signals such as dual humps, elevated resting potentials, and reduced action potential amplitudes near the reentrant core were actually due to photon scattering. The models also revealed that photon scattering can result in the underestimation of both virtual electrode polarization during an electrical shock and the number of phase singularities detected during VF.

Finally, computational models of the rabbit ventricles have made contributions to understanding electromechanical activity in the heart (Gurev et al., 2010; Trayanova et al.,

2011; Trayanova and Rice, 2011), however these are not reviewed here, consistent with the focus of the article on arrhythmogenesis.

VI. Conclusion

As this review demonstrates, computational studies utilizing the rabbit ventricles have made significant contributions in our current understanding of the mechanisms underlying ventricular arrhythmia induction, perpetuation, and termination. Rabbit ventricles served as the perfect animal model for the initial applications of 3D modeling due to its ability to accurately represent mammalian cardiac electrophysiology while being small enough to remain tractable even for computationally intensive bidomain simulations. However, recent increases in computational power have rendered feasible an array of more complex rabbit models of increased structural complexity, those that include the conduction system, microstructures, and structural and electrophysiological remodeling resulting from diseases such as myocardial infarction.

In the years to come, the development of more complex rabbit ventricular models will further enhance the utility of such models in elucidating cardiac electrical function. Such developments will rely on the models being broadened and expanded by the availability of experimental data on rabbit-specific cellular electrophysiological characteristics such as ion channel dynamics, intrinsic cellular and structural heterogeneities, and remodeling due to disease. These complex models can be used to bridge our understanding of rabbit electrical function from different spatial and temporal scales. For example, discovery about new ion channel dynamics or signaling pathways obtained from genetic or other studies can be easily incorporated in current 3D models to help test hypotheses related to the molecular determinants of 3D electrical function and its emerging properties.

Additionally, future rabbit models can incorporate experimental findings from different sources and modalities to constrain the models and ensure their predictive power. Complex 3D models that have been experimentally constrained and validated will potentially be used as a test bed for pharmacological studies and therapeutic improvements. The unique ability to block or modify specific currents or signaling pathways can lead to the use of rabbit models to help aid in designing and testing future anti-arrhythmic drugs. Rabbit ventricular modeling has also been at the forefront in the development of individualized, image-based modeling techniques, a methodology poised to revolutionize cardiac computational modeling. In summary, the works highlighted in this review underscore the importance of rabbit ventricular models in advancing our understanding of cardiac electrophysiology and in ushering the use of computational models in translational studies.

Limitations

One trend that can be noticed from the above summary is the increase in complexity and inclusion of rabbit-specific properties in the single cell and geometrical models of the rabbit ventricles. In general, the studies that were discussed in the review did not incorporate every rabbit specific detail at all scales. This is due to a variety of reasons, from unavailability of the rabbit specific AP model during the early 3D ventricular studies, computational tractability and available computer processing power, and the inclusion of only the specific

parameters that are necessary to address the hypothesis of the particular study. In the initial studies using the 3D UCSD rabbit ventricles, a generic AP model based on the guinea pig was used to represent ionic electrophysiology. The good concordance between the simulated results and experimental studies demonstrated that this provided a reasonable approximation of the rabbit electrophysiology (Rodriguez, Li et al. 2005). Additionally, most of the studies did not incorporate the Purkinje system due to the added computational cost of the highly detailed Purkinje models.

Due to current limitations in experimental techniques, some of the mechanisms discussed in the previous studies require further experimental validation. In particular, the difficulty of recording electrical activity at a high spatio-temporal resolution throughout the 3D ventricles has made confirmation of the role of highly detailed structural heterogeneity on electrical activity difficult to confirm.

References

- Aguel F, Eason J, Trayanova NA. Advances in modeling cardiac defibrillation. *Int J Bifurcat Chaos*. 2003; 13:3791–803.
- Antzelevitch C, Fish J. Electrical heterogeneity within the ventricular wall. *Basic Res Cardiol*. 2001; 96:517–27. [PubMed: 1177069]
- Arevalo H, Rodriguez B, Trayanova N. Arrhythmogenesis in the heart: Multiscale modeling of the effects of defibrillation shocks and the role of electrophysiological heterogeneity. *Chaos*. 2007; 17:015103. [PubMed: 17411260]
- Ashihara T, Constantino J, Trayanova NA. Tunnel propagation of postshock activations as a hypothesis for fibrillation induction and isoelectric window. *Circ Res*. 2008; 102:737–45. [PubMed: 18218982]
- Ashihara T, Haraguchi R, Nakazawa K, Namba T, Ikeda T, Nakazawa Y, Ozawa T, Ito M, Horie M, Trayanova NA. The role of fibroblasts in complex fractionated electrograms during persistent/permanent atrial fibrillation: implications for electrogram-based catheter ablation. *Circ Res*. 2012; 110:275–84. [PubMed: 22179057]
- Ashihara T, Trayanova NA. Asymmetry in membrane responses to electric shocks: insights from bidomain simulations. *Biophys J*. 2004; 87:2271–82. [PubMed: 15454429]
- Aslanidi OV, Sleiman RN, Boyett MR, Hancox JC, Zhang H. Ionic mechanisms for electrical heterogeneity between rabbit Purkinje fiber and ventricular cells. *Biophys J*. 2010; 98:2420–31. [PubMed: 20513385]
- Atkinson A, Inada S, Li J, Tellez JO, Yanni J, Sleiman R, Allah EA, Anderson RH, Zhang H, Boyett MR, Dobrzynski H. Anatomical and molecular mapping of the left and right ventricular His-Purkinje conduction networks. *J Mol Cell Cardiol*. 2011; 51:689–701. [PubMed: 21741388]
- Baher AA, Uy M, Xie F, Garfinkel A, Qu Z, Weiss JN. Bidirectional ventricular tachycardia: ping pong in the His-Purkinje system. *Heart Rhythm*. 2011; 8:599–605. [PubMed: 21118730]
- Behradfar E, Nygren A, Vigmond EJ. The role of Purkinje-myocardial coupling during ventricular arrhythmia: a modeling study. *PLoS One*. 2014; 9:e88000. [PubMed: 24516576]
- Benson A, Gilbert S, Ries M, Aslanidi O, Zhang H, Boyett M, Dobrzynski H, Holden A. 0.2 mm cubic voxel reconstruction of rabbit heart geometry and architecture using diffusion tensor magnetic resonance imaging. *Proc Physiol Soc*. 2008; 10:PC11.
- Berne P, Brugada J. Brugada syndrome 2012. *Circ J*. 2012; 76:1563–71. [PubMed: 22789973]
- Bishop MJ, Boyle PM, Plank G, Welsh DG, Vigmond EJ. Modeling the role of the coronary vasculature during external field stimulation. *IEEE Trans Biomed Eng*. 2010a; 57:2335–45. [PubMed: 20542762]
- Bishop MJ, Gavaghan DJ, Trayanova NA, Rodriguez B. Photon scattering effects in optical mapping of propagation and arrhythmogenesis in the heart. *J Electrocardiol*. 2007a; 40:S75–80. [PubMed: 17993334]

- Bishop MJ, Plank G. The role of fine-scale anatomical structure in the dynamics of reentry in computational models of the rabbit ventricles. *J Physiol.* 2012; 590:4515–35. [PubMed: 22753546]
- Bishop MJ, Plank G, Burton RA, Schneider JE, Gavaghan DJ, Grau V, Kohl P. Development of an anatomically detailed MRI-derived rabbit ventricular model and assessment of its impact on simulations of electrophysiological function. *Am J Physiol Heart Circ Physiol.* 2010b; 298:H699–718. [PubMed: 19933417]
- Bishop MJ, Plank G, Vigmond E. Investigating the role of the coronary vasculature in the mechanisms of defibrillation. *Circ Arrhythm Electrophysiol.* 2012; 5:210–9. [PubMed: 22157522]
- Bishop MJ, Rodriguez B, Eason J, Whiteley JP, Trayanova N, Gavaghan DJ. Synthesis of voltage-sensitive optical signals: application to panoramic optical mapping. *Biophys J.* 2006; 90:2938–45. [PubMed: 16443665]
- Bishop MJ, Rodriguez B, Qu F, Efimov IR, Gavaghan DJ, Trayanova NA. The role of photon scattering in optical signal distortion during arrhythmia and defibrillation. *Biophys J.* 2007b; 93:3714–26. [PubMed: 17978166]
- Bishop MJ, Vigmond EJ, Plank G. The functional role of electrophysiological heterogeneity in the rabbit ventricle during rapid pacing and arrhythmias. *Am J Physiol Heart Circ Physiol.* 2013; 304:H1240–52. [PubMed: 23436328]
- Bordas R, Gillow K, Lou Q, Efimov IR, Gavaghan D, Kohl P, Grau V, Rodriguez B. Rabbit-specific ventricular model of cardiac electrophysiological function including specialized conduction system. *Prog Biophys Mol Biol.* 2011; 107:90–100. [PubMed: 21672547]
- Bourn DW, Gray RA, Trayanova NA. Characterization of the relationship between preshock state and virtual electrode polarization-induced propagated graded responses resulting in arrhythmia induction. *Heart Rhythm.* 2006; 3:583–95. [PubMed: 16648066]
- Boyle PM, Deo M, Plank G, Vigmond EJ. Purkinje-mediated effects in the response of quiescent ventricles to defibrillation shocks. *Ann Biomed Eng.* 2010; 38:456–68. [PubMed: 19876737]
- Boyle PM, Masse S, Nanthakumar K, Vigmond EJ. Transmural IK(ATP) heterogeneity as a determinant of activation rate gradient during early ventricular fibrillation: mechanistic insights from rabbit ventricular models. *Heart Rhythm.* 2013a; 10:1710–7. [PubMed: 23948344]
- Boyle PM, Park CJ, Arevalo HJ, Vigmond EJ, Trayanova NA. Sodium current reduction unmasks a structure-dependent substrate for arrhythmogenesis in the normal ventricles. *PLoS One.* 2014; 9:e86947. [PubMed: 24489810]
- Boyle PM, Veenhuizen GD, Vigmond EJ. Fusion during entrainment of orthodromic reciprocating tachycardia is enhanced for basal pacing sites but diminished when pacing near Purkinje system end points. *Heart Rhythm.* 2013b; 10:444–51. [PubMed: 23207137]
- Boyle PM, Williams JC, Ambrosi CM, Entcheva E, Trayanova NA. A comprehensive multiscale framework for simulating optogenetics in the heart. *Nat Commun.* 2013c; 4:2370. [PubMed: 23982300]
- Burton RA, Plank G, Schneider JE, Grau V, Ahammer H, Keeling SL, Lee J, Smith NP, Gavaghan D, Trayanova N, Kohl P. Three-dimensional models of individual cardiac histoanatomy: tools and challenges. *Ann N Y Acad Sci.* 2006; 1080:301–19. [PubMed: 17132791]
- Camelliti P, Borg TK, Kohl P. Structural and functional characterisation of cardiac fibroblasts. *Cardiovasc Res.* 2005; 65:40–51. [PubMed: 15621032]
- Campos FO, Shiferaw Y, Prassl AJ, Boyle PM, Vigmond EJ, Plank G. Stochastic spontaneous calcium release events trigger premature ventricular complexes by overcoming electrotonic load. *Cardiovasc Res.* 2015; 107:175–83. [PubMed: 25969391]
- Cerrone M, Noujaim SF, Tolkacheva EG, Talkachou A, O'Connell R, Berenfeld O, Anumonwo J, Pandit SV, Vikstrom K, Napolitano C, Priori SG, Jalife J. Arrhythmogenic mechanisms in a mouse model of catecholaminergic polymorphic ventricular tachycardia. *Circ Res.* 2007; 101:1039–48. [PubMed: 17872467]
- Chen PS, Shibata N, Dixon EG, Martin RO, Ideker RE. Comparison of the defibrillation threshold and the upper limit of ventricular vulnerability. *Circulation.* 1986; 73:1022–8. [PubMed: 3698224]
- Cheng J, Kamiya K, Liu W, Tsuji Y, Toyama J, Kodama I. Heterogeneous distribution of the two components of delayed rectifier K⁺ current: a potential mechanism of the proarrhythmic effects of methanesulfonanilideclass III agents. *Cardiovasc Res.* 1999; 43:135–47. [PubMed: 10536698]

- Clayton RH, Zhuchkova EA, Panfilov AV. Phase singularities and filaments: simplifying complexity in computational models of ventricular fibrillation. *Prog Biophys Mol Biol.* 2006; 90:378–98. [PubMed: 16098568]
- Coghlan HC, Coghlan AR, Buckberg GD, Cox JL. ‘The electrical spiral of the heart’: its role in the helical continuum. The hypothesis of the anisotropic conducting matrix. *Eur J Cardiothorac Surg.* 2006; 29(1):S178–87. [PubMed: 16563785]
- Constantino J, Long Y, Ashihara T, Trayanova NA. Tunnel propagation following defibrillation with ICD shocks: hidden postshock activations in the left ventricular wall underlie isoelectric window. *Heart Rhythm.* 2010; 7:953–61. [PubMed: 20348028]
- Corrias A, Giles W, Rodriguez B. Ionic mechanisms of electrophysiological properties and repolarization abnormalities in rabbit Purkinje fibers. *Am J Physiol Heart Circ Physiol.* 2011; 300:H1806–13. [PubMed: 21335469]
- Deo M, Boyle P, Plank G, Vigmond E. Arrhythmogenic mechanisms of the Purkinje system during electric shocks: a modeling study. *Heart Rhythm.* 2009; 6:1782–9. [PubMed: 19959130]
- Deo M, Boyle PM, Kim AM, Vigmond EJ. Arrhythmogenesis by single ectopic beats originating in the Purkinje system. *Am J Physiol Heart Circ Physiol.* 2010; 299:H1002–11. [PubMed: 20622103]
- Deo M, Ruan Y, Pandit SV, Shah K, Berenfeld O, Blaufox A, Cerrone M, Noujaim SF, Denegri M, Jalife J, Priori SG. KCNJ2 mutation in short QT syndrome 3 results in atrial fibrillation and ventricular proarrhythmia. *Proc Natl Acad Sci U S A.* 2013; 110:4291–6. [PubMed: 23440193]
- Efimov IR, Aguel F, Cheng Y, Wollenzier B, Trayanova N. Virtual electrode polarization in the far field: implications for external defibrillation. *Am J Physiol Heart Circ Physiol.* 2000; 279:H1055–70. [PubMed: 10993768]
- Efimov IR, Cheng Y, Van Wagoner DR, Mazgalev T, Tchou PJ. Virtual electrode-induced phase singularity: a basic mechanism of defibrillation failure. *Circ Res.* 1998; 82:918–25. [PubMed: 9576111]
- Efimov IR, Nikolski VP, Salama G. Optical imaging of the heart. *Circ Res.* 2004; 95:21–33. [PubMed: 15242982]
- Fast VG, Kleber AG. Block of impulse propagation at an abrupt tissue expansion: evaluation of the critical strand diameter in 2- and 3-dimensional computer models. *Cardiovasc Res.* 1995a; 30:449–59. [PubMed: 7585837]
- Fast VG, Kleber AG. Cardiac tissue geometry as a determinant of unidirectional conduction block: assessment of microscopic excitation spread by optical mapping in patterned cell cultures and in a computer model. *Cardiovasc Res.* 1995b; 29:697–707. [PubMed: 7606760]
- Fedida D, Giles WR. Regional variations in action potentials and transient outward current in myocytes isolated from rabbit left ventricle. *J Physiol.* 1991; 442:191–209. [PubMed: 1665856]
- Fenton FH, Cherry EM, Karma A, Rappel WJ. Modeling wave propagation in realistic heart geometries using the phase-field method. *Chaos.* 2005; 15:13502. [PubMed: 15836267]
- Gemmell P, Burrage K, Rodriguez B, Quinn TA. Population of computational rabbit-specific ventricular action potential models for investigating sources of variability in cellular repolarisation. *PLoS One.* 2014; 9:e90112. [PubMed: 24587229]
- Gray RA, Pertsov AM, Jalife J. Spatial and temporal organization during cardiac fibrillation. *Nature.* 1998; 392:75–8. [PubMed: 9510249]
- Gurev V, Constantino J, Rice JJ, Trayanova NA. Distribution of electromechanical delay in the heart: insights from a three-dimensional electromechanical model. *Biophys J.* 2010; 99:745–54. [PubMed: 20682251]
- Haissaguerre M, Shoda M, Jais P, Nogami A, Shah DC, Kautzner J, Arentz T, Kalushe D, Lamaison D, Griffith M, Cruz F, de Paola A, Gaita F, Hocini M, Garrigue S, Macle L, Weerasooriya R, Clementy J. Mapping and ablation of idiopathic ventricular fibrillation. *Circulation.* 2002; 106:962–7. [PubMed: 12186801]
- Higham J, Aslanidi OV, Zhang H. Large speed increase using novel GPU based algorithms to simulate cardiac excitation waves in 3D rabbit ventricles. *Computing in Cardiology.* 2011; 38:9–12.
- Hill YR, Child N, Hanson B, Wallman M, Coronel R, Plank G, Rinaldi CA, Gill J, Smith NP, Taggart P, Bishop MJ. Investigating a Novel Activation-Repolarisation Time Metric to Predict Localised

- Vulnerability to Reentry Using Computational Modelling. *PLoS One*. 2016; 11:e0149342. [PubMed: 26934736]
- Hill, YR.; Plank, G.; Smith, NP.; Bishop, MJ. *Functional Imaging and Modeling of the Heart*. Springer; 2013. Comparison of changes in effective electrical size with activation rate between small mammalian and human ventricular models; p. 54-62.
- Hillebrenner MG, Eason JC, Trayanova NA. Mechanistic inquiry into decrease in probability of defibrillation success with increase in complexity of preshock reentrant activity. *Am J Physiol Heart Circ Physiol*. 2004; 286:H909–17. [PubMed: 14604852]
- Hooks DA, Berte B, Yamashita S, Mahida S, Sellal JM, Aljefairi N, Frontera A, Derval N, Denis A, Hocini M, Haissaguerre M, Jais P, Sacher F. New strategies for ventricular tachycardia and ventricular fibrillation ablation. *Expert Rev Cardiovasc Ther*. 2015; 13:263–76. [PubMed: 25666031]
- Husti Z, Tábori K, Juhász V, Hornyik T, Varró A, Baczkó I. Combined inhibition of key potassium currents has different effects on cardiac repolarization reserve and arrhythmia susceptibility in dogs and rabbits. *Can J Physiol Pharmacol*. 2015; 93:535–44. [PubMed: 25928472]
- Idriss SF, Wolf PD. Transmural action potential repolarization heterogeneity develops postnatally in the rabbit. *J Cardiovasc Electrophysiol*. 2004; 15:795–801. [PubMed: 15250865]
- Inada S, Hancox JC, Zhang H, Boyett MR. One-dimensional mathematical model of the atrioventricular node including atrio-nodal, nodal, and nodal-his cells. *Biophys J*. 2009; 97:2117–27. [PubMed: 19843444]
- Jacquemet V, Henriquez CS. Loading effect of fibroblast-myocyte coupling on resting potential, impulse propagation, and repolarization: insights from a microstructure model. *Am J Physiol Heart Circ Physiol*. 2008; 294:H2040–52. [PubMed: 18310514]
- Jie X, Gurev V, Trayanova N. Mechanisms of mechanically induced spontaneous arrhythmias in acute regional ischemia. *Circ Res*. 2010; 106:185–92. [PubMed: 19893011]
- Jie X, Rodriguez B, de Groot JR, Coronel R, Trayanova N. Reentry in survived subepicardium coupled to depolarized and inexcitable midmyocardium: insights into arrhythmogenesis in ischemia phase 1B. *Heart Rhythm*. 2008; 5:1036–44. [PubMed: 18598961]
- Jie X, Trayanova NA. Mechanisms for initiation of reentry in acute regional ischemia phase 1B. *Heart Rhythm*. 2010; 7:379–86. [PubMed: 20097623]
- Krishnamoorthi S, Perotti LE, Borgstrom NP, Ajijola OA, Frid A, Ponnaluri AV, Weiss JN, Qu Z, Klug WS, Ennis DB, Garfinkel A. Simulation Methods and Validation Criteria for Modeling Cardiac Ventricular Electrophysiology. *PLoS One*. 2014; 9:e114494. [PubMed: 25493967]
- Li W, Gurev V, McCulloch AD, Trayanova NA. The role of mechanoelectric feedback in vulnerability to electric shock. *Prog Biophys Mol Biol*. 2008; 97:461–78. [PubMed: 18374394]
- Li W, Janardhan AH, Fedorov VV, Sha Q, Schuessler RB, Efimov IR. Low-energy multistage atrial defibrillation therapy terminates atrial fibrillation with less energy than a single shock. *Circ Arrhythm Electrophysiol*. 2011; 4:917–25. [PubMed: 21980076]
- Li W, Kohl P, Trayanova N. Induction of ventricular arrhythmias following mechanical impact: a simulation study in 3D. *J Mol Histol*. 2004; 35:679–86. [PubMed: 15614623]
- Li W, Kohl P, Trayanova N. Myocardial ischemia lowers precordial thump efficacy: an inquiry into mechanisms using three-dimensional simulations. *Heart Rhythm*. 2006; 3:179–86. [PubMed: 16443533]
- Li W, Ripplinger CM, Lou Q, Efimov IR. Multiple monophasic shocks improve electrotherapy of ventricular tachycardia in a rabbit model of chronic infarction. *Heart Rhythm*. 2009; 6:1020–7. [PubMed: 19560090]
- Luther S, Fenton FH, Kornreich BG, Squires A, Bittihn P, Hornung D, Zabel M, Flanders J, Gladuli A, Campoy L, Cherry EM, Luther G, Hasenfuss G, Krinsky VI, Pumar A, Gilmour RF Jr, Bodenschatz E. Low-energy control of electrical turbulence in the heart. *Nature*. 2011; 475:235–9. [PubMed: 21753855]
- MacCannell KA, Bazzazi H, Chilton L, Shibukawa Y, Clark RB, Giles WR. A mathematical model of electrotonic interactions between ventricular myocytes and fibroblasts. *Biophys J*. 2007; 92:4121–32. [PubMed: 17307821]

- Mahajan A, Shiferaw Y, Sato D, Baher A, Olcese R, Xie LH, Yang MJ, Chen PS, Restrepo JG, Karma A, Garfinkel A, Qu Z, Weiss JN. A rabbit ventricular action potential model replicating cardiac dynamics at rapid heart rates. *Biophys J*. 2008; 94:392–410. [PubMed: 18160660]
- Maharaj T, Blake R, Trayanova N, Gavaghan D, Rodriguez B. The role of transmural ventricular heterogeneities in cardiac vulnerability to electric shocks. *Prog Biophys Mol Biol*. 2008; 96:321–38. [PubMed: 17915299]
- Maleckar MM, Greenstein JL, Giles WR, Trayanova NA. Electrotonic coupling between human atrial myocytes and fibroblasts alters myocyte excitability and repolarization. *Biophys J*. 2009a; 97:2179–90. [PubMed: 19843450]
- Maleckar MM, Greenstein JL, Giles WR, Trayanova NA. K⁺ current changes account for the rate dependence of the action potential in the human atrial myocyte. *Am J Physiol Heart Circ Physiol*. 2009b; 297:H1398–410. [PubMed: 19633207]
- Maleckar MM, Woods MC, Sidorov VY, Holcomb MR, Mashburn DN, Wikswo JP, Trayanova NA. Polarity reversal lowers activation time during diastolic field stimulation of the rabbit ventricles: insights into mechanisms. *Am J Physiol Heart Circ Physiol*. 2008; 295:H1626–33. [PubMed: 18708441]
- McDowell KS, Arevalo HJ, Maleckar MM, Trayanova NA. Susceptibility to arrhythmia in the infarcted heart depends on myofibroblast density. *Biophys J*. 2011; 101:1307–15. [PubMed: 21943411]
- Meunier JM, Eason JC, Trayanova NA. Termination of reentry by a long-lasting AC shock in a slice of canine heart: a computational study. *J Cardiovasc Electrophysiol*. 2002; 13:1253–61. [PubMed: 12521342]
- Meunier JM, Trayanova NA, Gray RA. Sinusoidal stimulation of myocardial tissue: effects on single cells. *J Cardiovasc Electrophysiol*. 1999; 10:1619–30. [PubMed: 10636192]
- Meunier JM, Trayanova NA, Gray RA. Entrainment by an extracellular AC stimulus in a computational model of cardiac tissue. *J Cardiovasc Electrophysiol*. 2001; 12:1176–84. [PubMed: 11699528]
- Mironov S, Jalife J, Tolkacheva EG. Role of conduction velocity restitution and short-term memory in the development of action potential duration alternans in isolated rabbit hearts. *Circulation*. 2008; 118:17–25. [PubMed: 18559701]
- Panfilov AV. Is heart size a factor in ventricular fibrillation? Or how close are rabbit and human hearts? *Heart Rhythm*. 2006; 3:862–4. [PubMed: 16818223]
- Pinto JM, Boyden PA. Electrical remodeling in ischemia and infarction. *Cardiovasc Res*. 1999; 42:284–97. [PubMed: 10533567]
- Plank G, Prassl A, Hofer E, Trayanova NA. Evaluating intramural virtual electrodes in the myocardial wedge preparation: simulations of experimental conditions. *Biophys J*. 2008; 94:1904–15. [PubMed: 17993491]
- Puglisi JL, Bers DM. LabHEART: an interactive computer model of rabbit ventricular myocyte ion channels and Ca transport. *Am J Physiol Cell Physiol*. 2001; 281:C2049–60. [PubMed: 11698264]
- Rantner LJ, Arevalo HJ, Constantino JL, Efimov IR, Plank G, Trayanova NA. Three-dimensional mechanisms of increased vulnerability to electric shocks in myocardial infarction: Altered virtual electrode polarizations and conduction delay in the peri-infarct zone. *J Physiol*. 2012; 590:4537–51. [PubMed: 22586222]
- Rantner LJ, Tice BM, Trayanova NA. Terminating ventricular tachyarrhythmias using far-field low-voltage stimuli: Mechanisms and delivery protocols. *Heart Rhythm*. 2013; 10:1209–17. [PubMed: 23628521]
- Robichaux RP, Dossall DJ, Osorio J, Garner NW, Li L, Huang J, Ideker RE. Periods of highly synchronous, non-reentrant endocardial activation cycles occur during long-duration ventricular fibrillation. *J Cardiovasc Electrophysiol*. 2010; 21:1266–73. [PubMed: 20487123]
- Rodriguez B, Eason JC, Trayanova N. Differences between left and right ventricular anatomy determine the types of reentrant circuits induced by an external electric shock. A rabbit heart simulation study. *Prog Biophys Mol Biol*. 2006; 90:399–413. [PubMed: 16055175]

- Rodriguez B, Li L, Eason JC, Efimov IR, Trayanova NA. Differences between left and right ventricular chamber geometry affect cardiac vulnerability to electric shocks. *Circ Res.* 2005; 97:168–75. [PubMed: 15976315]
- Rodriguez B, Tice B, Eason J, Aguel F, Trayanova N. Cardiac vulnerability to electric shocks during phase 1A of acute global ischemia. *Heart Rhythm.* 2004a; 6:695–703. [PubMed: 15851241]
- Rodriguez B, Tice BM, Eason JC, Aguel F, Ferrero JM Jr, Trayanova N. Effect of acute global ischemia on the upper limit of vulnerability: a simulation study. *Am J Physiol Heart Circ Physiol.* 2004b; 286:H2078–88. [PubMed: 14751853]
- Rodriguez B, Tice BM, Eason JC, Aguel F, Trayanova N. Cardiac vulnerability to electric shocks during phase 1A of acute global ischemia. *Heart Rhythm.* 2004c; 1:695–703. [PubMed: 15851241]
- Rodriguez B, Trayanova N. Upper limit of vulnerability in a defibrillation model of the rabbit ventricles. *J Electrocardiol.* 2003; (36 Suppl):51–6. [PubMed: 14716592]
- Rohr S. Myofibroblasts in diseased hearts: new players in cardiac arrhythmias? *Heart Rhythm.* 2009; 6:848–56. [PubMed: 19467515]
- Romero D, Sebastian R, Bijnens BH, Zimmerman V, Boyle PM, Vigmond EJ, Frangi AF. Effects of the purkinje system and cardiac geometry on biventricular pacing: a model study. *Ann Biomed Eng.* 2010; 38:1388–98. [PubMed: 20094915]
- Romero L, Carbonell B, Trenor B, Rodríguez B, Saiz J, Ferrero JM. Systematic characterization of the ionic basis of rabbit cellular electrophysiology using two ventricular models. *Prog Biophys Mol Biol.* 2011; 107:60–73. [PubMed: 21749896]
- Sachse FB, Moreno AP, Abildskov JA. Electrophysiological modeling of fibroblasts and their interaction with myocytes. *Ann Biomed Eng.* 2008; 36:41–56. [PubMed: 17999190]
- Samie FH, Berenfeld O, Anumonwo J, Mironov SF, Udassi S, Beaumont J, Taffet S, Pertsov AM, Jalife J. Rectification of the background potassium current: a determinant of rotor dynamics in ventricular fibrillation. *Circ Res.* 2001; 89:1216–23. [PubMed: 11739288]
- Sampson KJ, Henriquez CS. Electrotonic influences on action potential duration dispersion in small hearts: a simulation study. *Am J Physiol Heart Circ Physiol.* 2005; 289:H350–60. [PubMed: 15734889]
- Shannon TR, Wang F, Puglisi J, Weber C, Bers DM. A mathematical treatment of integrated Ca dynamics within the ventricular myocyte. *Biophys J.* 2004; 87:3351–71. [PubMed: 15347581]
- Shaw RM, Rudy Y. Electrophysiologic effects of acute myocardial ischemia: a theoretical study of altered cell excitability and action potential duration. *Cardiovasc Res.* 1997a; 35:256–72. [PubMed: 9349389]
- Shaw RM, Rudy Y. Ionic mechanisms of propagation in cardiac tissue. Roles of the sodium and L-type calcium currents during reduced excitability and decreased gap junction coupling. *Circ Res.* 1997b; 81:727–41. [PubMed: 9351447]
- Tandri H, Weinberg SH, Chang KC, Zhu R, Trayanova NA, Tung L, Berger RD. Reversible cardiac conduction block and defibrillation with high-frequency electric field. *Sci Transl Med.* 2011; 3:102ra96.
- Tice BM, Rodriguez B, Eason J, Trayanova N. Mechanistic investigation into the arrhythmogenic role of transmural heterogeneities in regional ischaemia phase 1A. *Europace.* 2007; 9(6):vi46–58. [PubMed: 17959693]
- Tranum-Jensen J, Wilde AA, Vermeulen JT, Janse MJ. Morphology of electrophysiologically identified junctions between Purkinje fibers and ventricular muscle in rabbit and pig hearts. *Circ Res.* 1991; 69:429–37. [PubMed: 1860183]
- Trayanova N, Li W, Eason J, Kohl P. Effect of stretch-activated channels on defibrillation efficacy. *Heart Rhythm.* 2004; 1:67–77. [PubMed: 15851121]
- Trayanova N, Skouibine K, Moore P. Virtual electrode effects in defibrillation. *Prog Biophys Mol Biol.* 1998; 69:387–403. [PubMed: 9785947]
- Trayanova NA, Constantino J, Gurev V. Electromechanical models of the ventricles. *Am J Physiol Heart Circ Physiol.* 2011; 301:H279–86. [PubMed: 21572017]
- Trayanova NA, Rice JJ. Cardiac electromechanical models: from cell to organ. *Front Physiol.* 2011; 2:43. [PubMed: 21886622]

- Vadakkumpadan F, Arevalo H, Prassl AJ, Chen J, Kicking F, Kohl P, Plank G, Trayanova N. Image-based models of cardiac structure in health and disease. *Wiley Interdiscip Rev Syst Biol Med*. 2010; 2:489–506. [PubMed: 20582162]
- Vadakkumpadan F, Rantner LJ, Tice B, Boyle P, Prassl AJ, Vigmond E, Plank G, Trayanova N. Image-based models of cardiac structure with applications in arrhythmia and defibrillation studies. *J Electrocardiol*. 2009; 42:157 e1–10. [PubMed: 19181330]
- Varró A, Lathrop DA, Hester SB, Nánási PP, Papp JG. Ionic currents and action potentials in rabbit, rat, and guinea pig ventricular myocytes. *Basic Res Cardiol*. 1993; 88:93–102. [PubMed: 8389123]
- Vasquez C, Mohandas P, Louie KL, Benamer N, Bapat AC, Morley GE. Enhanced fibroblast-myocyte interactions in response to cardiac injury. *Circ Res*. 2010; 107:1011–20. [PubMed: 20705922]
- Vetter FJ, McCulloch AD. Three-dimensional analysis of regional cardiac function: a model of rabbit ventricular anatomy. *Prog Biophys Mol Biol*. 1998; 69:157–83. [PubMed: 9785937]
- Vigmond EJ, Clements C. Construction of a computer model to investigate sawtooth effects in the Purkinje system. *IEEE Trans Biomed Eng*. 2007; 54:389–99. [PubMed: 17355050]
- Weinberg SH, Chang KC, Zhu R, Tandri H, Berger RD, Trayanova NA, Tung L. Defibrillation success with high frequency electric fields is related to degree and location of conduction block. *Heart Rhythm*. 2013; 10:740–8. [PubMed: 23354078]
- Xie F, Qu Z, Garfinkel A, Weiss JN. Electrophysiological heterogeneity and stability of reentry in simulated cardiac tissue. *Am J Physiol Heart Circ Physiol*. 2001; 280:H535–45. [PubMed: 11158949]
- Xie Y, Sato D, Garfinkel A, Qu Z, Weiss JN. So little source, so much sink: requirements for afterdepolarizations to propagate in tissue. *Biophys J*. 2010; 99:1408–15. [PubMed: 20816052]
- Xu X, Rials SJ, Wu Y, Salata JJ, Liu T, Bharucha DB, Marinchak RA, Kowey PR. Left ventricular hypertrophy decreases slowly but not rapidly activating delayed rectifier potassium currents of epicardial and endocardial myocytes in rabbits. *Circulation*. 2001; 103:1585–90. [PubMed: 11257089]
- Zamiri N, Masse S, Ramadeen A, Kusha M, Hu X, Azam MA, Liu J, Lai PF, Vigmond EJ, Boyle PM, Behradfar E, Al-Hesayen A, Waxman MB, Backx P, Dorian P, Nanthakumar K. Dantrolene improves survival after ventricular fibrillation by mitigating impaired calcium handling in animal models. *Circulation*. 2014; 129:875–85. [PubMed: 24403563]
- Zicha S, Moss I, Allen B, Varro A, Papp J, Dumaine R, Antzelevich C, Nattel S. Molecular basis of species-specific expression of repolarizing K⁺ currents in the heart. *Am J Physiol Heart Circ Physiol*. 2003; 285:H1641–9. [PubMed: 12816752]
- Gemmell P, Burrage K, Rodriguez B, Quinn TA. Rabbit-specific computational modelling of ventricular cell electrophysiology: using population models to explore variability to ischemia. *Prog Biophys Mol Biol*. 2016 in press, this issue.
- Teh I, Burton RAB, McClymont D, Capel RA, Aston D, Kohl P, Schneider JE. Mapping Cardiac Microstructure of Rabbit Heart in Different Mechanical States by High Resolution Diffusion Tensor Imaging. *Prog Biophys Mol Biol*. 2016 in press, this issue.

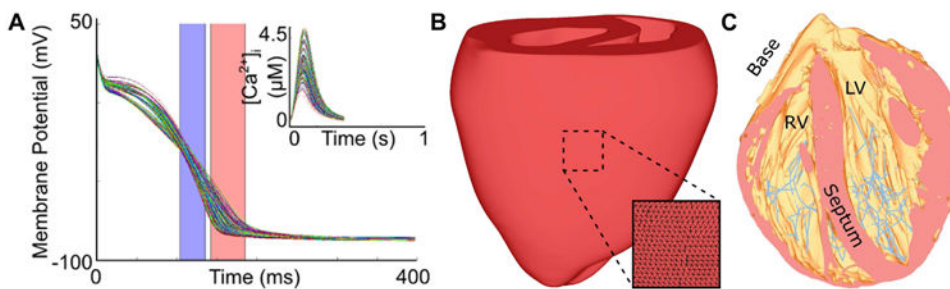


Fig. 1. Multi-scale modeling of rabbit cardiac electrophysiology. (A) Family of simulated rabbit ventricular myocyte APs and intracellular calcium ($[Ca^{2+}]_i$) transients, produced using the model by Mahajan, Shiferaw et al. (Mahajan et al., 2008). Physiologically-relevant variability in shape and duration was achieved by using hundreds of stochastically-generated parameter combinations to modify behavior of repolarizing currents (Gemmell et al., 2014). APD50 and APD90 ranges are shown as blue and red shaded areas, respectively. (Reprinted with permission from (Gemmell et al., 2014)). (B) UC San Diego rabbit heart geometry with tetrahedral element edges shown in inset. (C) Structurally-detailed rabbit mesh of the rabbit ventricles including an image-based representation of the free-running Purkinje system (pink). (Reprinted with permission from (Vadakkumpadan et al., 2009))

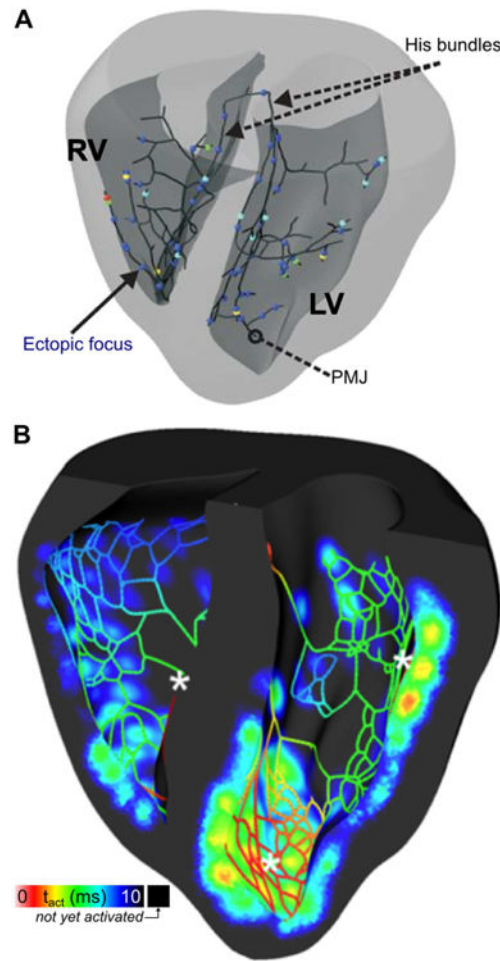


Fig. 2. Premature ventricular contractions (PVCs) originating in the Purkinje system (PS). (A) 3D map showing locations of initial excitation that triggered PVCs in a model of the rabbit PS and ventricles. All cells in the model were prone to delayed afterdepolarization (DAD)-induced excitation due to spontaneous calcium release, but such activity occurred exclusively in the PS due to lower source-sink mismatch. PMJ = Purkinje-myocardial junction. (Reprinted with permission from Ref (Campos et al., 2015)) (B) 3D map showing activation times in a cutaway view of the rabbit ventricles and PS during a post-pause propagating response caused by DAD. Asterisks show locations where DADs occurred in the PS, leading to propagating excitation that eventually caused a PVC. (Reprinted with permission from (Zamiri et al., 2014))

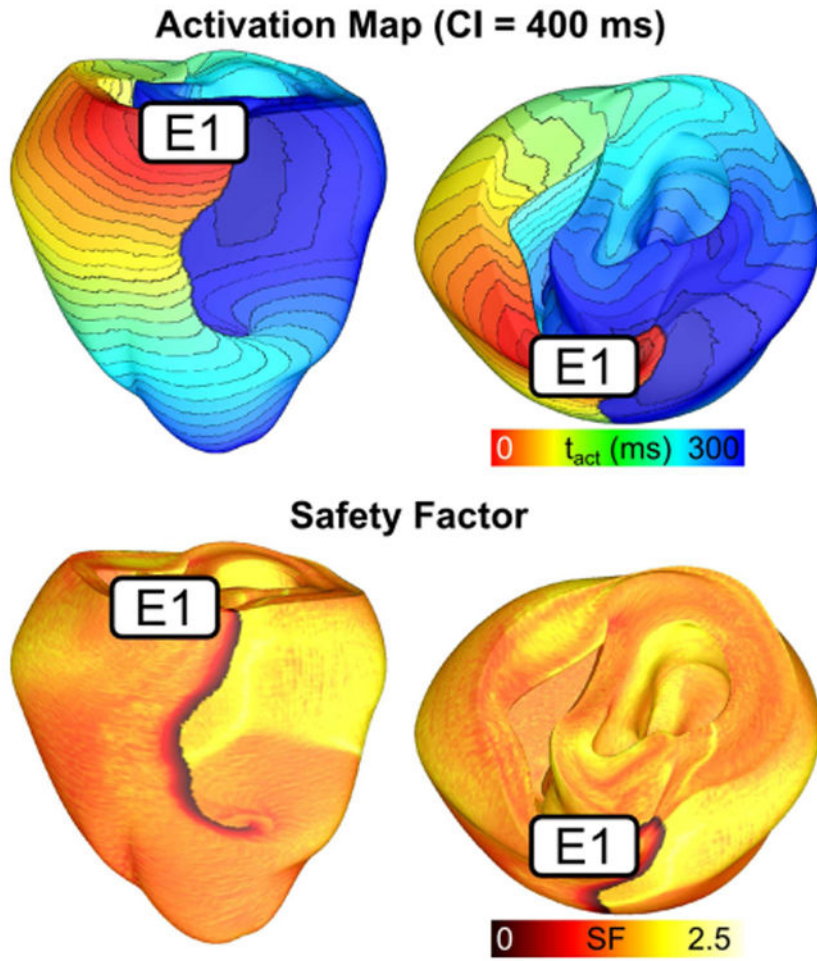


Fig. 3. Reentry induction due to structural heterogeneity and decreased sodium channel expression. Activation maps showing reentry induced via pacing from an electrode (E1) located on the RV outflow tract. The corresponding safety factor map show that areas with critically low SF (<1) corresponds with site of conduction block at the RVOT insertion point. (Modified and reprinted with permission from (Boyle et al., 2014))

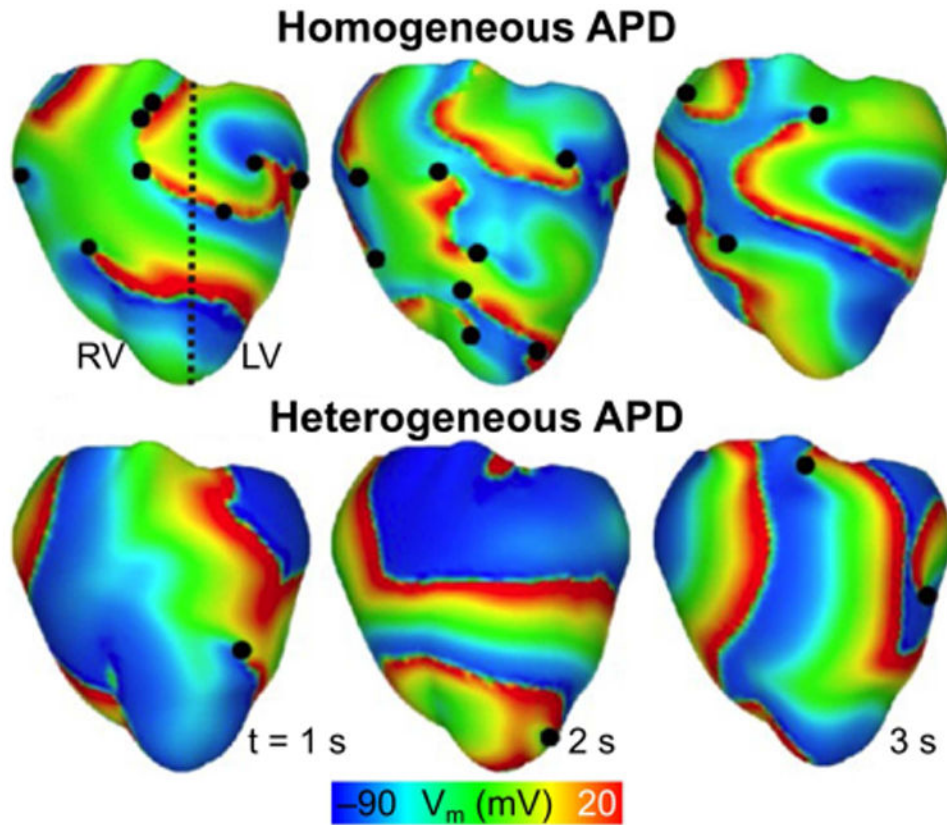


Fig. 4. Role of LV/RV APD heterogeneity on VF dynamics. Transmembrane potential distributions during VF for model with heterogeneous APD (i.e. left, LV, and right, RV, ventricles have different APDs) and for model with homogenous APD. The dashed black line denotes the border between regions characterized by a different APD. Epicardial phase singularities are marked with solid black circles. (Modified and reprinted with permission from Ref (Arevalo et al., 2007))

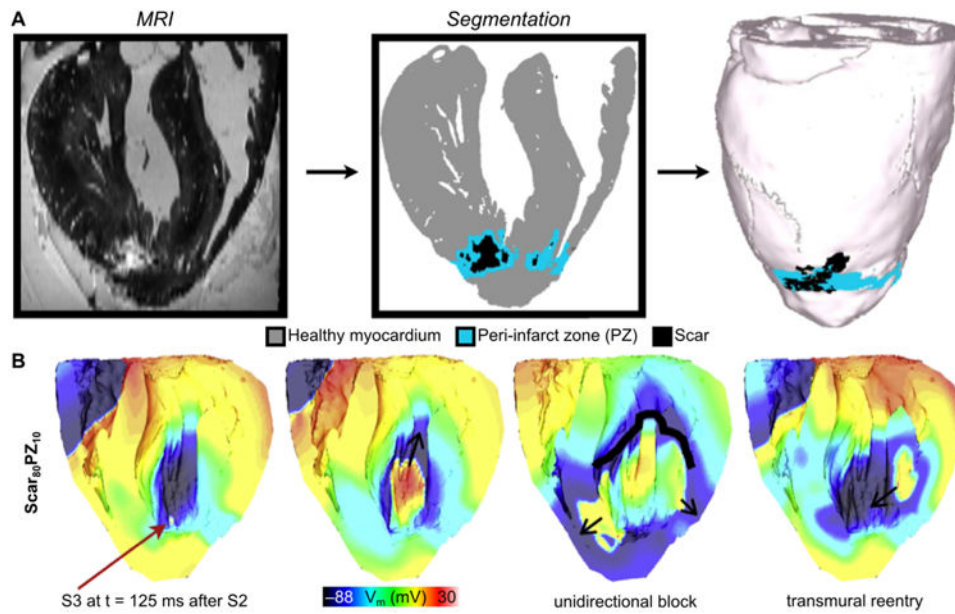


Fig. 5. Post-infarction arrhythmogenesis. (A) High-resolution MRI-based model of the infarcted rabbit ventricle with fibroblasts incorporated in the zone of infarct. (B) Coupling of fibroblasts to myocytes (80% in the scar and 10% in the PZ) results in arrhythmia. Red arrow indicates the location of the premature activation. (Modified and reprinted with permission from (McDowell et al., 2011))

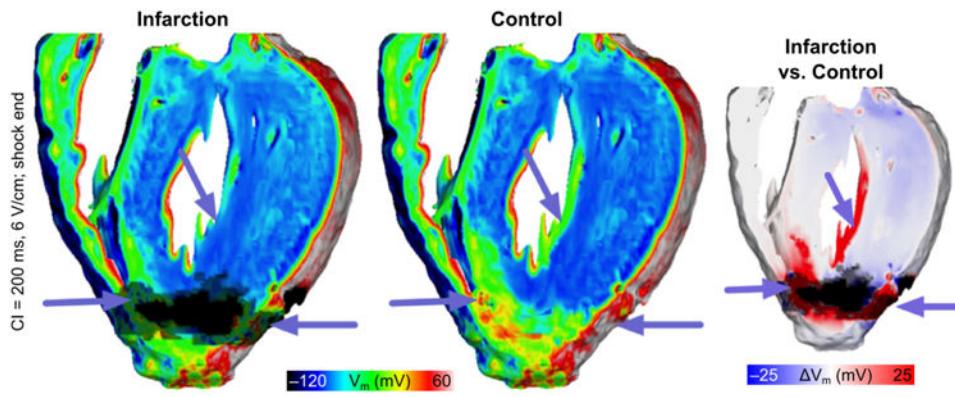


Fig. 6. Vulnerability to shock-induced arrhythmia in rabbits with healed infarction. Distribution of shock-end V_m show less tissue was excited in the infarction model (purple arrows). Right-most panel shows the V_m difference between infarction and control models, computed as control V_m minus infarction V_m . (Reprinted with permission from (Rantner et al., 2012))